

Title Page

Pharmacologic inhibition of site-1 protease activity inhibits SREBP processing and reduces lipogenic enzyme gene expression and lipid synthesis in cultured cells and experimental animals

Julie L. Hawkins, Michael D. Robbins, Laurie C. Warren, Donghui Xia, Stephen F. Petras, James J. Valentine, Alison H. Varghese, Ing-Kae Wang, Timothy A. Subashi, Lorraine D. Shelly, Bruce A. Hay, Katherine T. Landschulz, Kieran F. Geoghegan, and H. James Harwood, Jr

Department of Cardiovascular and Metabolic Diseases (J.L.H., M.D.R., L.C.W., D.X., S.F.P., L.D.S., K.T.L., H.J.H.), Department of Exploratory Medicinal Sciences (J.J.V, A.H.V., I.W., T.A.S., B.A.H., K.F.G.), Pfizer Global Research and Development, Groton/New London Laboratories, Eastern Point Road, Groton, CT 06340

Running Title Page

Running title: Inhibition of SREBP site-1 protease

Address correspondence to: Dr. Julie Hawkins, Department of Cardiovascular and Metabolic Diseases, Pfizer Global Research and Development, Groton/New London Laboratories, Eastern Point Road, Groton, CT 06340. Telephone: (860)441-4235. FAX: (860)686-1176. E-mail: julie.l.hawkins@pfizer.com

Number of text pages: 33

Number of tables: 0

Number of figures: 4

Number of references: 27

Number of words in Abstract: 203

Number of words in Introduction: 728

Number of words in Discussion: 956

ABBREVIATIONS: SREBP, sterol regulatory element-binding protein; S1P, SREBP site-1 protease; S2P, SREBP site-2 protease; SCAP, SREBP cleavage-activating protein; Insig-1, Insulin-induced gene-1; LXR, liver X receptor; ER, endoplasmic reticulum; COPII, coat complex II; PMSF, phenylmethanesulfonyl fluoride; CHO, Chinese Hamster Ovary

Cardiovascular section

ABSTRACT

Sterol regulatory element-binding proteins (SREBPs) are major transcriptional regulators of cholesterol, fatty acid and glucose metabolism. Genetic disruption of SREBP activity reduces plasma and liver levels of cholesterol and triglycerides, as well as insulin-stimulated lipogenesis, suggesting that SREBP is a viable target for pharmacological intervention. The proprotein convertase SREBP site-1 protease (S1P) is an important post-transcriptional regulator of SREBP activation. This report demonstrates that 10 μ M PF-429242, a recently described reversible, competitive aminopyrrolidineamide inhibitor of S1P, inhibits endogenous SREBP processing in Chinese hamster ovary cells. The same compound also down-regulates the signal from an SRE-luciferase reporter gene in HEK293 cells and the expression of endogenous SREBP target genes in cultured HepG2 cells. In HepG2 cells, PF-429242 inhibited cholesterol synthesis with an IC₅₀ of 0.5 μ M. In mice treated with PF-429242 for 24 h, the expression of hepatic SREBP target genes was suppressed, and the hepatic rates of cholesterol and fatty acid synthesis were reduced. Taken together, these data establish that small molecule S1P inhibitors are capable of reducing cholesterol and fatty acid synthesis *in vivo*, and therefore represent a potential new class of therapeutic agents for dyslipidemia and for a variety of cardiometabolic risk factors associated with diabetes, obesity and the metabolic syndrome.

Introduction

Sterol regulatory element-binding proteins (SREBPs) are major transcriptional regulators of cholesterol, fatty acid and glucose biosynthesis. There are three major forms of SREBP. SREBP-1a and SREBP-1c preferentially regulate fatty acid synthesis, while SREBP-2 preferentially regulates sterol synthesis (Horton et al., 2002). All SREBPs are transcriptionally auto-regulated. SREBP-1a and SREBP-1c are encoded by a single gene, but the expression of each is regulated by a different promoter and they differ in their N-terminal regions as a result of alternative processing (Shimomura et al., 1997). SREBP-1c is also transcriptionally regulated by insulin and LXR (Repa et al., 2000).

Each SREBP is synthesized as an endoplasmic reticulum integral membrane protein with two transmembrane domains, one ER lumenal loop, and cytosolic C-terminal and N-terminal domains (Brown and Goldstein, 1997). Translocation of membrane-bound SREBP from the ER to the cis-Golgi and the subsequent cleavage events in the Golgi comprise major points of regulation in the generation of active SREBP, requiring SREBP cleavage activating protein (SCAP), the recently characterized factors Insig-1 and Insig-2 (Engelking et al., 2005), and two processing enzymes, SREBP site-1 protease (S1P) and SREBP site-2 protease (S2P) (Brown and Goldstein, 1997).

SREBP processing is regulated intracellularly by cholesterol and oxysterols. When the sterol content is high, cholesterol-bound SCAP associates with the SREBP C-terminal cytoplasmic domain to form a complex that binds to oxysterol-bound Insig (Radhakrishnan et al., 2004). This association with Insig blocks the transport of SCAP/SREBP from the ER to the Golgi, where the SREBP processing enzymes S1P and

S2P, reside (Sun et al., 2005; Sun et al., 2007). In low-sterol conditions, the SREBP-SCAP complex is released from Insig, and SREBP is escorted by SCAP, sorted into COPII vesicles and transported to the Golgi, where the two proteases effect two sequential cleavages of SREBP. S1P cleaves SREBP at the loop inside the lumen of the Golgi, and this cleavage must occur before the second cleavage, which is catalyzed by S2P within the first transmembrane domain. This event releases active SREBP, which subsequently migrates to the nucleus, binds to sterol response elements (SREs) of cholesterol and fatty acid biosynthetic target genes, and activates their transcription.

The SREBPs, especially SREBP-1c, are up-regulated in response to many pharmacological and physiological stimulations. Increased SREBP-1c contributes to the elevated rates of hepatic fatty acid synthesis that leads to steatosis in diabetic mice (Browning and Horton, 2004). Inhibition of SREBP processing can overcome up-regulation of SREBP expression, leading to down-regulation of cholesterol and fatty acid synthesis (Engelking et al., 2004). Currently, there is no evidence for differential regulation of the three SREBPs through the proteolytic activation process. Over expression of Insig and deletion of SCAP or S1P result in down-regulation of all SREBP target genes (Engelking et al., 2004; Matsuda et al., 2001; Yang et al., 2001) including the SREBP genes themselves (Yang et al., 2001). In S1P and SCAP liver-specific knockout mice, expression levels of SREBP target genes were decreased and the animals had lower levels of liver and plasma cholesterol and triglyceride compared to wild type mice (Matsuda et al., 2001; Yang et al., 2001). These results suggested that inhibitors of SREBP processing could be effective agents to reduce hepatic and plasma cholesterol and triglyceride levels *in vivo*.

S1P is a serine protease that belongs to the proprotein convertase (PC) family (Sakai et al., 1998), but is a rather untypical member (Henrich et al., 2005). Its proform is expressed as a type II membrane bound protein. As with most enzymes in the PC family, S1P undergoes autoprocessing of its proform and becomes a mature enzyme that resides in the cis-Golgi. After initial signal peptidase-catalyzed cleavage at site A (Gly22-Asp23), S1P is further processed sequentially at site B (Lys137-Tyr138) and site C (Leu186-Arg187) (Espenshade et al., 1999). After proteolytic processing, the resultant catalytically competent S1P cleaves SREBPs following their lumen loop sequence of - Arg-Ser-Val-Leu- (Duncan et al., 1997). A soluble form of S1P with its transmembrane and cytosol domain deleted was shown to possess S1P catalytic activities, which could be inhibited by PMSF (Cheng et al., 1999).

We recently described the identification of a reversible and competitive small molecule inhibitor of S1P activity, the aminopyrrolidineamide PF-429242 (Hay et al., 2007). In this report we describe the effects of PF-429242 on the processing of SREBP, on the expression of SREBP target genes, and on sterol and fatty acid synthesis in cultured cells and in experimental animals.

Methods

S1P expression and purification – Residue numbering for human S1P follows Swiss-Prot accession Q14703. S1P protein was expressed and purified using a Chinese Hamster Ovary (CHO) cell expression system. The expression vector for soluble site-1 protease (sS1P) was generated by cloning a human site-1 protease cDNA encoding amino acids 17-997, encompassing the pro-, catalytic and cysteine-rich domains (Espenshade et al., 1999) into the pSecTag/FRT/V5-His vector (Invitrogen, #K6025-01). The resulting plasmid was transfected into Flp-In CHO cells (Invitrogen, #R758-07) following the manufacturer's instructions. Individual clones of stable cells overexpressing soluble S1P (sS1P) were isolated and maintained in DMEM growth medium (Invitrogen, #11995-065) containing 10% FBS (Invitrogen, #16140-071), 2 mM L-glutamine (Invitrogen, #25030-081), 1% Pen/Strep (Invitrogen, #15070-063), and 500 µg/ml Hygromycin B (Invitrogen, #10687-010). For large scale protein expression, the Flp-In CHO/sS1P cells were adapted to suspension growth by stepwise reduction of the FBS concentration in IS-CHO (Irvine Scientific, #91109) serum-free medium containing 500 µg/ml Hygromycin B. Wave Bioreactors (Wave Biotech, System 20 or System 20/50EH) were inoculated at $\sim 3.5 \times 10^5$ cells/ml, and operated at 25 rocks per minute and 0.2 l/minute aeration with 5% CO₂ at 37°C. Conditioned medium was harvested at 7 days by refrigerated continuous flow centrifugation (Heraeus Contifuge) at 3500 x g. Leupeptin (Sigma, #L9783) and 1 M Tris HCl (Biosolutions, #BIO850-18, pH 8.0) were added at 1 mg/l and 25 ml/L, respectively. Harvested conditioned medium was passed through a 0.2 µm filter and stored at 4°C until purification.

Conditioned medium was concentrated five-fold with a GE Kwick Cassette concentrator (MWCO 10K, GE Healthcare) using a peristaltic pump at 100 rpm (Watson Marlow, Model 603S). Concentrated medium was then diafiltered with 5 volumes of 25 mM Tris HCl, 1 mM CaCl₂, pH 8.0, and mixed with Ni²⁺-Sepharose resin (GE Healthcare) equilibrated with 25 mM Tris HCl, pH 8.0. After overnight binding at 4°C, the resin was packed into a Pharmacia XK26 column. The column was mounted on an AKTA Explorer chromatography system (GE Healthcare) and washed with 25 mM Tris HCl, pH 8.0, followed by Buffer A (25 mM Tris HCl, pH 8.0, 1 mM CaCl₂, 1 M NaCl, 10% glycerol (JT Baker, #2136-01)). Further sequential washes were then carried out with increasing concentrations of imidazole (10 mM, 20 mM and 30 mM; Calbiochem ULTROL grade, #4015) in Buffer B (25 mM Tris HCl, 1 mM CaCl₂, 10% glycerol, pH 8.0) before the column was finally eluted with Buffer B containing 200 mM imidazole. The eluate was then concentrated seven-fold in a Vivascience 20 ml concentrator (polyethersulfone, 5K MWCO; Vivascience, #VS2011), mixed with an equal volume of glycerol and stored at -20°C. Aliquots of all fractions were analyzed by SDS-PAGE and Western blotting with anti-V5 antibody (Invitrogen, #46-0708) to identify fractions containing sS1P.

Enzymatic assay for S1P - The primary assay was based on the fluorogenic substrate, Ac-VFRSLK-MCA (Peptides International, code: MCA-3679-PI), as described (Cheng et al., 1999; Hay et al., 2007). Alternative fluorogenic substrates for S1P were based on previously described simple peptide substrates (Cheng et al., 1999; Toure et al., 2000). Each peptide was modified with a dabcyI group at the N-terminus and with tetramethylrhodamine (TMR) near the C-terminus. The fluorescence of the TMR was

statically quenched by contact with the dabcyl group when the substrates were intact, but enzyme-catalyzed cleavage eliminated quenching. The substrates were (i) Dabcyl-Ser-Gly-Ser-Gly-Arg-Ser-Val-Leu-Ser-Phe-Glu-Ser-Gly-Ser-Lys(TMR)-Arg-OH, from site-1 of SREBP-2 and (ii) Dabcyl-Arg-His-Ser-Ser-Arg-Arg-Leu-Leu-Arg-Ala-Leu-Glu-Gly-Gly-Lys(TMR)-OH, from site B of S1P. Substrates were produced as custom orders by AnaSpec Inc, San Jose, CA 95131. Assays with these substrates were conducted at 37°C in a PerSeptive Biosystems CytoFluor 4000 96-well fluorescence plate reader using 4 µM substrate in 0.025 M Tris acetate, 1 mM CaCl₂, pH 8.0 (at 22°C), with the 530 nm excitation filter and 620 nm emission filter in line.

SREBP-2 Western blot - To test for the inhibition of endogenous SREBP processing by an S1P inhibitor, western blotting for the membrane and nuclear forms of SREBP-2 was performed as previously described with minor modifications (DeBose-Boyd et al., 1999; Sakai et al., 1996). 2 x 10⁶ CHO cells were grown in a 10 cm plate in DMEM/F12 (Invitrogen, #11320-033) with 5% FCS and Penicillin-Streptomycin (Invitrogen, #15140-122). After overnight culture in an incubator at 37°C with 5% CO₂, cells were switched to DMEM/F12 with 5% (v/v) delipidated FBS (Cocalico Biologicals, Inc. #54-0116) containing 10 µg/ml cholesterol and 1 µg/ml 25-hydroxycholesterol or different concentrations of PF-429242 for 24 h. One hour before cells were harvested for protein extraction, α-N-acetyl-Leu-Leu-Nle-CHO (ALLN) (Calbiochem, #208719) was added to the medium at a final concentration of 25 µg/ml.

After harvest, cells from each plate were spun down in PBS, then resuspended in 400 µl of ice-cold Buffer C (10 mM HEPES/KOH pH 7.6, 10 mM KCl, 1.5 mM MgCl₂, 1 mM EDTA, 1 mM EGTA, 250 mM sucrose) with freshly added 1 mM DTT and protease

inhibitors (pepstatin A 5 µg/ml, leupeptin 10 µg/ml, Pefabloc 0.5 mM, aprotinin 2.8 µg/ml, ALLN 25 µg/ml). Remaining procedures were performed on ice. To shear DNA, the cells were passed thirty times through a 23 gauge needle mounted on a 1 ml syringe. The lysate was centrifuged at 1100 x g for 7 min at 4°C, and the resulting supernatant was centrifuged again at 100,000 x g for 45 min at 4°C in an ultracentrifuge. The pellet containing membrane-bound forms of SREBP was resuspended in 35 µl of SDS-lysis buffer (10 mM Tris HCl, 100 mM NaCl, 1% SDS, 1 mM EDTA, 1 mM EGTA, pH 6.8). To recover nuclear SREBP, the pellet from the 1100 x g spin was suspended in 0.1 ml of ice cold Buffer D (20 mM HEPES/KOH, 420 mM NaCl, 1.5 mM MgCl₂, 2.5% glycerol, 1 mM EDTA, 1 mM EGTA, pH 7.6) with freshly added protease inhibitors as described above. Pellets were rocked at 4°C for 1-2 h, after which the samples were centrifuged at 100,000 x g for 45 min at 4°C. The resulting supernatant contained nuclear SREBP.

45 µg nuclear extract or 25 µg membrane fraction were loaded on Criterion XT Tris-Acetate 3-8% gels (BioRad, #345-0129) and subjected to electrophoresis at 150-175 V for about 1 h. Proteins were then transferred to nitrocellulose membranes using a Trans-Blot SD Semi-Dry Transfer Cell (BioRad, #170-3940) at 20 V for 45 min. The resulting blots were blocked in PBS/10 % milk/0.05% Tween overnight at 4°C. The next day, blots were incubated with 5 µg/ml IgG-7D4, a monoclonal antibody directed against the N-terminal region of hamster SREBP-2 (ATCC, hybridoma cell line CRL-2198) (Yang et al., 1995) in PBS/10% milk/0.05% Tween on a shaker at room temperature for 2 h, followed by four washes of 10 min each with PBS/T. The blots then were incubated for 1 h with donkey anti-mouse HRP (Jackson ImmunoResearch Lab, #715-035-150) diluted at 1:50,000 in PBS/milk/Tween, and then washed four times for 10 min each

with PBS/T. The blots were developed with LumiLight PLUS Western Blotting substrate (Roche Applied Science, #2015200).

SRE-Luciferase reporter assay – SRE-regulated luciferase constructs were generated by inserting the sterol response element SRE-38 into commercial luciferase expression vectors. Several such vectors were tested, including pLuc-MCS (SRE-TATA, Stratagene, #219087), pTAL-Luc (SRE-TK, Clontech, #631909) and pGL2-enhancer (SRE-SV40, Promega, #E1621). The SRE-38 sequence was designed on the basis of published sequence information (Dawson et al., 1988). A *Bam* HI restriction site sequence was added at the end of the oligonucleotides to facilitate cloning. Two complementary oligonucleotides (SRE-38 sense: gatcCTTGAAAATCACCCCACTGTGGGATCCTCCCCCTGCTG; SRE-38 antisense: gatcCAGCAGGGGGAGGATCCCACAGTGGGGTGATTTTCAAG) were annealed and the double-stranded SRE-38 was inserted into each plasmid at a *Bgl* II site. SRE-38 insertions were confirmed by sequencing analysis.

For the assay of SRE-luciferase, HEK293T cells were placed in a 96-well plate at 40,000 cells per well on the day before transfection. Cells were transfected using Lipofectamine 2000 with 40 ng SRE-luciferase and 2 ng of a HSV-TK regulated *Renilla* luciferase control construct (phRL-TK, Promega, #E6241), according to the manufacturer's instructions. One hour after transfection, cell culture media were replaced with 10% delipidated serum (LPDS)/DMEM containing either compounds in DMSO, or DMSO alone. After overnight exposure to compound, both luciferase activities were measured using the Dual-Luciferase Reporter Assay System (Promega

E1910). The ratio between firefly luciferase activity and *Renilla* luciferase activity obtained reflected SRE-specific compound effects on transcription.

Quantitation of SREBP target gene expression - The effects of compounds on the expression of SREBP target genes were evaluated in HepG2 cells. HepG2 cells were plated in 24-well plates at 300,000 cells/well and incubated overnight in 10% LPDS/DMEM at 37°C, 5% CO₂. The next day, cells were treated in triplicates with PF-429242 in 10% LPDS/DMEM for 24 h. Total RNA was isolated from each well with an RNeasy Mini Kit (Qiagen, #74106) following the manufacturer's instructions. On-column DNase treatment was performed with RNase-free DNase (Qiagen, #79254).

To test the *in vivo* efficacy of PF-429242 in regulating SREBP target genes, male CD1 mice (n=6) were dosed intraperitoneally with 10 or 30 mg/kg PF-429242 or saline once every 6 over a 24 h period. Mice were euthanized 6 h after the final dose and liver tissue was collected, frozen rapidly in liquid N₂ and stored at -80°C. For RNA isolation, 50-100 mg of frozen liver tissue from each sample was homogenized in 1 ml Trizol reagent (Invitrogen, #15596-026). Total RNA was extracted following the manufacturer's instructions, and the resulting total RNA from each sample underwent DNA-free treatment (DNA-free kit, Ambion, #1906).

Quantitative PCR analysis was performed for RNAs from individual cell culture wells (n=3) and individual mouse livers (n=6) as previously described. 1 µg of total RNA was used in 50 µl reverse transcription reactions using Applied Biosystems Taqman Reverse Transcription Reagent (ABI, #N808-0234). For each sample, the same RT product was used for all subsequent quantitative PCR reactions. Real-time quantitative PCR primer sets were based on published sequences (Liang et al., 2002; Yang et al.,

2001). Quantitative PCR reactions were performed using ABI SYBR Green PCR Master Mix (ABI, #4309155) with an ABI 7700 instrument. The expression levels of HMG-CoA reductase, fatty acid synthase, LDL receptor and ABCA1 were normalized with cyclophilin and presented as average plus standard deviation for individual RNA samples.

Quantitation of cholesterol and fatty acid synthesis– Cholesterol and fatty acid synthesis were evaluated in HepG2 cells by measuring incorporation of [2-¹⁴C]acetate into cellular lipids as previously described (Harwood, Jr. et al., 2003), but with the following modifications to allow simultaneous assessment of both cholesterol and fatty acid synthesis. HepG2 cells were plated in 24-well plates at 1.2×10^5 cells/well and incubated at 37°C, 5% CO₂. Cells reaching 70%-80% confluency were switched to 10% LPDS /DMEM. The next day, cells were treated with PF-429242 in 0.5 ml of 10% LPDS /DMEM at the indicated concentrations. Twenty-four hours after treatment, 25 µl of media containing 4 µCi of [2-¹⁴C]acetate (Amersham CFA14, 56 mCi/mmol) was added to each well and the plates were incubated at 37°C for 6 h. After incubation, the cells were dissolved in 0.5 ml of 0.2 N KOH and an aliquot was taken for protein determination. The remaining dissolved cells were combined with the media for extraction. [1,2-³H]cholesterol (50,000 dpm/tube, Amersham TRK330, 38 Ci/mmol) and 150 µg of cholesterol were added as count and thin-layer-chromatography (TLC)-visualizable internal standards, respectively. Samples were saponified by the addition of 0.30 ml of 50% KOH and 2.0 ml of ethanol, followed first by incubation for 2 h at 75°C and then by overnight incubation at room temperature. The saponified mixtures were extracted 3 times with 4.5 ml hexane. The pooled organic fractions were dried under N₂,

resuspended in 40 μ L of chloroform-hexane (1:1), and spotted onto plastic-backed PE-Sil G TLC plates for development in hexane-diethyl ether-acetic acid (70:30:2, v/v). The region indicated by the cholesterol standard was cut out, placed in 7 ml of Aquasol-2 liquid scintillation fluid, and counted on a Beckman LS6500 liquid scintillation counter.

After collection and assessment of the hexane fraction containing cholesterol, the remaining aqueous phase (containing fatty acid sodium salts) was acidified to pH<2 by addition of 0.5 ml of 12 M HCl. 100 μ g linoleic acid was added to each sample as a standard for TLC visualization. The resulting mixtures were then transferred to glass conical tubes and extracted three times with 4.5 ml hexane. The pooled organic fractions were dried under N₂, resuspended in 50 μ L of chloroform-hexane (1:1) and applied to plastic-backed PE-Sil G TLC plates for development in hexane-diethyl ether-acetic acid (90:30:1, v/v). The region indicated by the linoleic acid standard was cut out, placed in 7 ml of Aquasol-2 liquid scintillation fluid, and counted on a Beckman LS6500 liquid scintillation counter. Cholesterol and fatty acid synthesis are expressed as dpm [2-¹⁴C]acetate incorporated into either non-saponifiable or saponifiable lipids per mg cellular protein during the 6 h incubation at 37°C.

To detect changes in rates of sterol and fatty acid synthesis in response to PF-429242 treatment *in vivo*, we measured the incorporation of [2-¹⁴C]acetate into sterols and fatty acids as previously described (Harwood, Jr. et al., 1997). Male CD1 mice (n=10) were dosed intraperitoneally with PF-429242 at 10 mg/kg and 30 mg/kg or saline once every 6 h over a 24 h period. Five hours after the final dose, mice were given a 0.2 ml intraperitoneal injection of [2-¹⁴C]acetate. One hour after the administration of radiolabel, mice were euthanized by asphyxiation with CO₂ and 0.75 g of liver was

removed and saponified at 70°C for 2 h in 1.3 ml of 2.5 N NaOH. After saponification, 2.5 ml of absolute ethanol was added to each sample, and the samples were mixed and allowed to stand overnight. The nonsaponifiable lipids were extracted twice by adding 4.8 ml of petroleum ether to each sample, shaking vigorously and then centrifuging at 1000 x g in a benchtop centrifuge for 5 min. The pooled organic fractions were transferred to liquid scintillation vials, dried down under N₂, dissolved in 7 ml of Aquasol-2 liquid scintillation fluid, and assessed for radioactivity using a Beckman LS6500 liquid scintillation counter.

After removal of the non-saponifiable lipids, the remaining aqueous layer (containing fatty acid sodium salts) was acidified to pH<2 by addition of 0.6 ml of 12 M HCl and extracted twice with 4.8 ml of petroleum ether. The pooled organic fractions were analyzed in the same way as for non-saponifiable lipids described above. Cholesterol and fatty acid synthesis are expressed as dpm [2-¹⁴C]acetate incorporated into either non-saponifiable or saponifiable lipids during the interval between [2-¹⁴C]acetate injection and CO₂ asphyxiation.

Studies using experimental animals – All procedures using experimental animals were approved by the institutional Animal Care and Use Procedures Review Board. CD1 mice were given food (RMH3200) and water ad libitum and treated intraperitoneally with either saline (vehicle) or saline containing PF-429242 as outlined above.

Results

A soluble recombinant form of site-1 protease (sS1P) in which residues 17-997 of the human protein were linked with C-terminal V5 and hexahistidine tags was purified by metal-affinity chromatography from conditioned medium of CHO cells overexpressing sS1P. The transmembrane and cytosolic domains of S1P (residues 998-1052) were absent from this product (Sakai et al., 1998), which was caused to be a secreted protein by replacing the native signal sequence with that of IgK. N-Terminal sequence analysis of purified sS1P gave a result of Arg-Ala-Ile-Pro-Arg, corresponding to the “C-form” of S1P (Espenshade et al., 1999). Propeptides (14 kDa and 6 kDa forms) were also detected in purified sS1P, although the percentage of purified sS1P that remained associated with propeptide was not determined. The yield of sS1P averaged 1 mg/L of conditioned medium, but a large fraction of this protein was aggregated or otherwise inactive. Despite this, the presence of activity demonstrating all the properties expected for S1P allowed screening to proceed.

High throughput screening for inhibitors of S1P led to identification of three hits with micromolar potency. Combinatorial synthesis of analogs around one of these hits generated Compound A (Hay et al., 2007), a racemic aminopyrrolidineamide S1P inhibitor with an IC₅₀ of 393 nM (Fig. 1A). Upon resolution it was found that the less potent enantiomer (Compound B; IC₅₀ = 971 nM) possessed the S stereochemistry whereas the more potent enantiomer (PF-429242) possessed the R stereochemistry. PF-429242 was shown to be a reversible, competitive S1P inhibitor which has an IC₅₀ of 175 nM in the MCA assay for sS1P (Fig. 1A). Testing against a panel of serine proteases indicated that PF-429242 was a highly selective inhibitor of S1P (Hay et al., 2007).

The secondary enzymatic assay was performed using alternative fluorogenic substrates based on two previously reported peptide substrates of S1P, corresponding to SREBP-2 site1 and S1P autocleavage site B (Cheng et al., 1999). Unlike the substrate for the high throughput screen, the secondary substrates contained amino-acid residues on both sides of the scissile bond. Cleavage by S1P was shown to occur at the Leu-Ser bond in the first substrate and at the Leu-Arg bond in the second. Compounds tested exhibited the same relative potency against both the primary and secondary substrates (data not shown).

S1P inhibitors should inhibit processing of SREBP, and reduce or prevent formation of the nuclear form of SREBP. As there is no evidence that S1P acts differentially upon SREBP-1 and SREBP-2, the fate of SREBP-2 in cells treated with PF-429242 was used as an indicator of the compound's ability to affect SREBP processing. Western blotting was used to analyze the respective levels of the nuclear and membrane-bound forms of SREBP-2 (Fig. 1B). In the absence of sterol, the nuclear form of SREBP-2 was predominant and the membrane form was much less abundant, indicating that proteolytic processing of SREBP was favored (Fig. 1B, lane 1). In the presence of sterol, SREBP-2 remained in the ER in its membrane-bound form, and the nuclear form of SREBP-2 was present at a much lower level (Fig. 1B, lane 2). A 10 μ M concentration of PF-429242 blocked the processing of endogenous SREBP-2 in CHO cells in the absence of sterol, as indicated by a much lower level of the nuclear form of SREBP-2 (Fig. 1B, lane 3). Similar inhibition of SREBP-2 processing by PF-429242 was also observed in HepG2 cells (data not shown).

The nuclear forms of SREBP regulate their target genes by binding to sterol response elements (SRE) and stimulating transcription. Inhibition of SREBP processing should therefore cause the expression of SRE-regulated genes to be downregulated. To test the ability of PF-429242 to downregulate SREBP transcriptional activity, SRE-luciferase reporter constructs were generated. Of three SRE-luciferase constructs tested in transfected HEK293 cells, SRE-TATA luciferase (based on the pLuc-MCS vector) was selected for the assay because it gave the largest percentage of inhibition when sterol was added to the culture medium. DNA sequencing confirmed that the SRE-TATA luciferase construct had two copies of the SRE 38 sequence connected head-to-tail and inserted into pLuc-MCS (Fig. 2A). In HEK293 cells transfected with the SRE-TATA luciferase construct, SREs are regulated by endogenous SREBPs; therefore, the assay was done in the presence of delipidated serum (LPDS) to induce endogenous SREBP activity. Increased concentrations of PF-429242 gave dose dependent inhibition of luciferase activity (Fig. 2B), suggesting that the compound was inhibiting the processing of endogenous SREBP to their nuclear forms. The luciferase activity was inhibited by up to 93% at 30 μ M PF-429242, with an IC₅₀ of 1.8 μ M. The inhibitory profiles of Compounds C and D, two related analogs of PF-429242 are also shown in Fig. 2B and the structures of these compounds in Fig. 2C.

The ability of PF-429242 to affect the expression of SREBP target genes in cultured cells was evaluated by treating HepG2 cells with 1, 3, 10 and 30 μ M PF-429242 for 24 h in DMEM/LPDS. The expression of endogenous SREBP target genes was tested by real-time quantitative PCR, using HMG-CoA synthase and fatty acid synthase to represent genes involved in sterol and fatty acid synthesis. Both genes were

downregulated in a dose-dependent fashion by PF-429242, with maximum inhibition of 95% for HMG-CoA synthase and 80% for fatty acid synthase at 3 μ M PF-429242 (Fig. 3A). The expression of LDL receptor, another SREBP target gene, was also downregulated (Fig. 3B), albeit less effectively than either HMG-CoA synthase or fatty acid synthase (e.g. 30% reduction in LDL receptor gene expression at a concentration of 1 μ M PF-429242 versus 60% inhibition of HMG-CoA synthase and fatty acid synthase gene expression at the same inhibitor concentration; Fig. 3 A and B). Inhibition of gene expression in HepG2 cells was observed under both 10% LPDS and 10% FBS-containing culture conditions (data not shown). The expression of a non-SREBP target gene, ABCA1, was not affected by PF-429242 (Fig. 3C), indicating that the reductions in expression of the SREBP target genes were not due to cytotoxicity of the compound, an observation confirmed by the absence of LDH release with compound treatment.

To evaluate the ability of PF-429242 to inhibit cholesterol and fatty acid synthesis in cultured cells, HepG2 cells were treated with 0.03, 0.1, 0.3, 1, 3 and 10 μ M PF-429242 for 24 h. Cells were then incubated with [2- 14 C]acetate for 6 h, and the incorporation of [2- 14 C]acetate into cholesterol and fatty acids was determined. The rate of cholesterol synthesis was inhibited by PF-429242 in a dose-dependent manner, with an IC_{50} = 0.53 μ M (Fig. 3D). Under these experimental conditions, however, there was no significant inhibition of fatty acid synthesis.

The short term *in vivo* efficacy of PF-429242 was tested in mice by measuring its effect on the expression of SREBP target genes and the rate of lipid synthesis in the liver. Because of its high clearance rate (75 ml/min/kg) and poor oral bioavailability (~5%) (Hay et al., 2007), mice were dosed intraperitoneally with either 10 mg/kg or 30 mg/kg

PF-429242 at 6 h intervals for 24 h. This dose was chosen to allow continuous exposure levels at or exceeding compound IC₅₀ for S1P over the time period tested. After this regimen, the level of HMG-CoA synthase RNA in mouse liver was downregulated by 72% (**p < 0.01) and 83% (**p<0.01), and fatty acid synthase expression was reduced by 41% (not statistically significant) and 77% (**p<0.01), in the 10 mg/kg and 30 mg/kg dosing groups, respectively (Fig. 4A). LDL receptor gene expression was also reduced by treatment, but, as observed in HepG2 cell-based assays, to a much lesser extent (20% reduction (not statistically significant) in the 10 mg/kg treated group and 30% reduction (**p<0.01) in the 30 mg/kg treated) than the expression of either lipogenic enzyme (Fig. 4A).

Consistent with the reductions in HMG-CoA synthase and fatty acid synthase gene expression, the rates of cholesterol and fatty acid synthesis were also decreased *in vivo* by short-term treatment with PF-429242. Incorporation of [2-¹⁴C]acetate into cholesterol was decreased by 40% (p=0.062) and 75% (***p<0.001) at 10 mg/kg and 30 mg/kg doses, respectively, as compared to vehicle-treated mice (Fig. 4B). Incorporation of [2-¹⁴C]acetate into fatty acid was reduced by 34% (not statistically significant) and 78% (***p<0.001), respectively (Fig. 4C).

Discussion

Western blotting of subcellular fractions from cells treated with PF-429242 provided the most direct evidence of S1P inhibition-mediated effects on SREBP. The relative abundance of nuclear and membrane-bound SREBP was distinctly different after PF-429242 treatment as compared to cells incubated with sterols. In the presence of excess sterol, the SCAP/SREBP complex remains in the ER. SREBP is not exposed to S1P, and therefore is not processed. Under the culture conditions utilized, high levels of sterols resulted in the expected decrease of nuclear SREBP and an increase in membrane-bound SREBP, while low sterol conditions resulted in increased nuclear and decreased membrane SREBP (Fig 1B). In contrast, treatment of cells with PF-429242 led to a marked change in the relative abundance of nuclear and membrane-bound forms of SREBP as compared to sterol-treated cells. This observation is consistent with the downregulation of SREBP gene expression after S1P inhibition, based on observations previously reported in S1P knockout mice (Yang et al., 2001). In these animals, both SREBP-1 and SREBP-2 precursors as well as nuclear forms of SREBP are greatly reduced, and this reduction is accompanied by a reduction in both SREBP-1 and SREBP-2 mRNA levels. Because expression of the SREBPs is also regulated by the nuclear forms of the SREBPs themselves, through SRE elements in their promoters, the reduction of precursor SREBP levels in these animals occurs as a consequence of downregulation of SREBP expression (Yang et al., 2001). In our experiments, SREBP-1 mRNA levels in HepG2 cells treated with 10 μ M PF-429242 were also reduced by 61%, consistent with a secondary downregulation of SREBP gene expression in response to S1P inhibition, and similar to that observed in the S1P knockout mice (Yang et al., 2001).

Another major player in the regulation of SREBP processing is SCAP. Reduction in nuclear and membrane SREBPs is also observed in SCAP knockout mice (Matsuda et al., 2001). Based on the results from our cell and animal efficacy studies, we can not rule out the possibility that our compounds might also have inhibited SCAP action. However, the close correlation between the potency of inhibitors in the S1P enzymatic assay and in the SRE-luciferase reporter expression assay across the series of S1P inhibitors suggests that SREBP processing inhibition as a result of S1P enzyme inhibition is the most probable explanation.

While *in vitro* proteolytic cleavage assays had initially yielded an IC₅₀ of 175 nM, PF-429242 inhibited the expression of SRE-luciferase in transfected HEK293 cells with an IC₅₀ of 1.85 μ M. LDL receptor message levels were reduced approximately 50% at this same concentration. In contrast, when expression levels of the endogenous SREBP targets HMG-CoA synthase and fatty acid synthase were quantitated by real-time PCR in HepG2 cells, PF-429242 had a somewhat higher potency, with an EC₅₀ < 1 μ M for both genes. Maximal reduction in RNA expression was also clearly gene-specific, with HMG-CoA synthase inhibited essentially completely (>95%) and fatty acid synthase inhibited only about 80% at 30 μ M concentration. We have tested multiple small molecule S1P inhibitors, and compared their ability to inhibit HMG-CoA synthase and fatty acid synthase by real-time RT-PCR. All the compounds tested followed the same order of potency for inhibition of both target genes. Given that differential reduction in cholesterol and fatty acid biosynthetic gene activity has also been observed in the published SREBP, S1P, and SCAP knockout mice genetic models (Shimano et al., 1997; Matsuda et al., 2001; Yang et al., 2001), these results potentially reflect the differential

interaction of SREBP family with the complex promoters of these genes and raise the possibility of “dialing in” relatively more cholesterol and fatty acid biosynthetic inhibition than LDL receptor reduction with this mechanism. Our results do suggest, however, that all compounds tested inhibited the processing of SREBP-1 and SREBP-2 to similar extents, with no indication that S1P preferentially cleaves one SREBP rather than another.

Because SREBP regulate multiple genes in cholesterol and fatty acid synthesis pathways (Horton et al., 2002), the inhibition of cholesterol and fatty acid synthesis should reflect the overall results of inhibiting many steps in the synthesis pathways. Potential lowering of LDL receptor is considered a major caveat of any mechanism aimed at disrupting SREBP, including S1P inhibition. Overall, acute treatment with PF-429242 yielded results highly reminiscent of the previously published S1P knockout mouse, including effects on hepatic cholesterol, fatty acid biosynthesis, and lowered LDL receptor levels (Yang et al., 2001). Despite this significant LDL receptor lowering, S1P knockout mice demonstrated reduced plasma cholesterol and triglyceride levels. Unfortunately, we were unable to test plasma cholesterol and triglyceride changes after prolonged treatment with compound due to the extremely poor pharmacokinetic properties of our compound. While definitive results await the identification of a more bioavailable and *in vivo* stable chemical tool, it is encouraging that cell-based data supports the possibility of differential regulation of target genes, with cholesterol and fatty acid biosynthetic target genes relatively more sensitive to reduced nuclear SREBP levels than the LDL receptor.

Despite its pharmacokinetic limitations, PF-429292 has enabled key cellular proof of mechanism and initial *in vivo* proof of concept studies for a new class of therapeutic agents. Taken together, these findings confirm the potential of S1P inhibitors to exhibit a profile which combines the benefits of a cholesterol synthesis inhibitor (e.g. HMG-CoA reductase inhibitor) with the benefits of a fatty acid metabolism modulator (e.g. acetyl-CoA carboxylase inhibitor). New medicines from this class would be potentially useful not only for patients with dyslipidemia, but also for those with a variety of cardiometabolic risk factors associated with insulin resistance, diabetes, obesity and the metabolic syndrome. Clearly, a compound with improved pharmacokinetic properties that could be administered chronically to experimental animals is required to further confirm that the inhibition of S1P activity would indeed possess these combined benefits.

References

- Brown MS and Goldstein JL (1997) The SREBP pathway: regulation of cholesterol metabolism by proteolysis of a membrane-bound transcription factor. *Cell* **89**:331-340.
- Browning JD and Horton JD (2004) Molecular mediators of hepatic steatosis and liver injury. *J Clin Invest* **114**:147-152.
- Cheng D, Espenshade PJ, Slaughter CA, Jaen JC, Brown MS, and Goldstein JL (1999) Secreted site-1 protease cleaves peptides corresponding to luminal loop of sterol regulatory element-binding proteins. *J Biol Chem* **274**:22805-22812.
- Dawson PA, Hofmann SL, van der Westhuyzen DR, Sudhof TC, Brown MS, and Goldstein JL (1988) Sterol-dependent repression of low density lipoprotein receptor promoter mediated by 16-base pair sequence adjacent to binding site for transcription factor Sp1. *J Biol Chem* **263**:3372-3379.
- DeBose-Boyd RA, Brown MS, Li WP, Nohturfft A, Goldstein JL, and Espenshade PJ (1999) Transport-dependent proteolysis of SREBP: relocation of site-1 protease from Golgi to ER obviates the need for SREBP transport to Golgi. *Cell* **99**:703-712.
- Duncan EA, Brown MS, Goldstein JL, and Sakai J (1997) Cleavage site for sterol-regulated protease localized to a Leu-Ser bond in the luminal loop of sterol regulatory element-binding protein-2. *J Biol Chem* **272**:12778-12785.
- Engelking LJ, Kuriyama H, Hammer RE, Horton JD, Brown MS, Goldstein JL, and Liang G (2004) Overexpression of Insig-1 in the livers of transgenic mice inhibits

SREBP processing and reduces insulin-stimulated lipogenesis. *J Clin Invest* **113**:1168-1175.

Engelking LJ, Liang G, Hammer RE, Takaishi K, Kuriyama H, Evers BM, Li WP, Horton JD, Goldstein JL, and Brown MS (2005) Schoenheimer effect explained-feedback regulation of cholesterol synthesis in mice mediated by Insig proteins. *J Clin Invest* **115**:2489-2498.

Espenshade PJ, Cheng D, Goldstein JL, and Brown MS (1999) Autocatalytic processing of site-1 protease removes propeptide and permits cleavage of sterol regulatory element-binding proteins. *J Biol Chem* **274**:22795-22804.

Harwood HJ, Jr., Barbacci-Tobin EG, Petras SF, Lindsey S, and Pellarin LD (1997) 3-(4-chlorophenyl)-2-(4-diethylaminoethoxyphenyl)-A-pentenitrile monohydrogen citrate and related analogs. Reversible, competitive, first half-reaction squalene synthetase inhibitors. *Biochem Pharmacol* **53**:839-864.

Harwood HJ, Jr., Petras SF, Shelly LD, Zaccaro LM, Perry DA, Makowski MR, Hargrove DM, Martin KA, Tracey WR, Chapman JG, Magee WP, Dalvie DK, Soliman VF, Martin WH, Mularski CJ, and Eisenbeis SA (2003) Isozyme-nonselective N-substituted bipiperidylcarboxamide acetyl-CoA carboxylase inhibitors reduce tissue malonyl-CoA concentrations, inhibit fatty acid synthesis, and increase fatty acid oxidation in cultured cells and in experimental animals. *J Biol Chem* **278**:37099-37111.

Hay BA, Abrams B, Zumbunn AY, Valentine JJ, Warren LC, Petras SF, Shelly LD, Xia A, Varghese AH, Hawkins JL, Van Camp JA, Robbins MD, Landschulz K, and Harwood

HJ, Jr. (2007) Aminopyrrolidineamide inhibitors of site-1 protease. *Bioorg Med Chem Lett* **17**:4411-4414

Henrich S, Lindberg I, Bode W, and Than ME (2005) Proprotein convertase models based on the crystal structures of furin and kexin: explanation of their specificity. *J Mol Biol* **345**:211-227.

Horton JD, Goldstein JL, and Brown MS (2002) SREBPs: activators of the complete program of cholesterol and fatty acid synthesis in the liver. *J Clin Invest* **109**:1125-1131.

Liang G, Yang J, Horton JD, Hammer RE, Goldstein JL, and Brown MS (2002) Diminished hepatic response to fasting/refeeding and liver X receptor agonists in mice with selective deficiency of SREBP-1c. *J Biol Chem* **277**:9520-9528

Matsuda M, Korn BS, Hammer RE, Moon YA, Komuro R, Horton JD, Goldstein JL, Brown MS, and Shimomura I (2001) SREBP cleavage-activating protein (SCAP) is required for increased lipid synthesis in liver induced by cholesterol deprivation and insulin elevation. *Genes Dev* **15**:1206-1216.

Radhakrishnan A, Sun LP, Kwon HJ, Brown MS, and Goldstein JL (2004) Direct binding of cholesterol to the purified membrane region of SCAP: mechanism for a sterol-sensing domain. *Mol Cell* **15**:259-268.

Repa JJ, Liang G, Ou J, Bashmakov Y, Lobaccaro JM, Shimomura I, Shan B, Brown MS, Goldstein JL, and Mangelsdorf DJ (2000) Regulation of mouse sterol regulatory element-binding protein-1c gene (SREBP-1c) by oxysterol receptors, LXR α and LXR β . *Genes Dev* **14**:2819-2830.

Sakai J, Duncan EA, Rawson RB, Hua X, Brown MS, and Goldstein JL (1996) Sterol-regulated release of SREBP-2 from cell membranes requires two sequential cleavages, one within a transmembrane segment. *Cell* **85**:1037-1046.

Sakai J, Rawson RB, Espenshade PJ, Cheng D, Seegmiller AC, Goldstein JL, and Brown MS (1998) Molecular identification of the sterol-regulated luminal protease that cleaves SREBPs and controls lipid composition of animal cells. *Mol Cell* **2**:505-514.

Shimano H, Shimomura I, Hammer RE, Herz J, Goldstein JL, Brown MS, and Horton JD (1997) Elevated levels of SREBP-2 and cholesterol synthesis in livers of mice homozygous for a targeted disruption of the SREBP-1 gene. *J Clin Invest* **100**:2115-2124.

Shimomura I, Shimano H, Horton JD, Goldstein JL, and Brown MS (1997) Differential expression of exons 1a and 1c in mRNAs for sterol regulatory element binding protein-1 in human and mouse organs and cultured cells. *J Clin Invest* **99**:838-845.

Sun LP, Li L, Goldstein JL, and Brown MS (2005) Insig required for sterol-mediated inhibition of Scap/SREBP binding to COPII proteins in vitro. *J Biol Chem* **280**:26483-26490.

Sun LP, Seemann J, Goldstein JL, and Brown MS (2007) Sterol-regulated transport of SREBPs from endoplasmic reticulum to Golgi: Insig renders sorting signal in Scap inaccessible to COPII proteins. *Proc Natl Acad Sci U S A* **104**:6519-6526.

Toure BB, Munzer JS, Basak A, Benjannet S, Rochemont J, Lazure C, Chretien M, and Seidah NG (2000) Biosynthesis and enzymatic characterization of human SKI-1/S1P and the processing of its inhibitory prosegment. *J Biol Chem* **275**:2349-2358.

Yang J, Brown MS, Ho YK, and Goldstein JL (1995) Three different rearrangements in a single intron truncate sterol regulatory element binding protein-2 and produce sterol-resistant phenotype in three cell lines. Role of introns in protein evolution. *J Biol Chem* **270**:12152-12161.

Yang J, Goldstein JL, Hammer RE, Moon YA, Brown MS, and Horton JD (2001) Decreased lipid synthesis in livers of mice with disrupted Site-1 protease gene. *Proc Natl Acad Sci U S A* **98**:13607-13612.

Footnotes

Present addresses:

K.T. Landschulz, Department of Translational Medicine and Pharmacogenomics, Eli Lilly
and Co.; landschulzkt@lilly.com

H. J. Harwood, Jr., Delphi BioMedical Consultants, LLC; h.james.harwood@gmail.com

Legends for Figures

Fig. 1. Inhibition of site-1 protease by PF-429242. (A) sS1P enzymatic activity assay.

1 μ g purified soluble S1P protein and 20 μ M Ac-VFRSLK-MCA were incubated at 37°C with compounds or vehicle for 4 h as described in Methods. Residual sS1P activity in presence of compounds is presented as percentage of S1P activity obtained with vehicle only (% inhibition). The inhibitory profiles of PF-429242, the racemate containing PF-429242 and its S enantiomer (Compound A), and the purified S enantiomer (Compound B) are shown. Data are the average of triplicate determinations \pm SD. Inset: The structure of PF-429242. (B) Western blot for SREBP-2 processing in culture cells.

Membrane protein and nuclear protein fractions were isolated from CHO cells cultured in the presence or absence of sterol and with or without PF-429242 for 24 h. Protein extracts were analyzed by western blotting followed by immunodetection with the anti-SREBP2 antibody 7D4. Top panel: 25 μ g membrane protein per lane; bottom panel: 45 μ g nuclear protein per lane. Lane 1: delipidated serum without compound; lane 2: 1 μ g/ml 25-hydroxycholesterol and 10 μ g/ml cholesterol added to delipidated serum; lane 3: delipidated serum with 10 μ M PF-429242.

Fig. 2. SRE-luciferase assay for SREBP activity. (A) The SRE-TATA-luciferase

construct. Two copies of the double-stranded SRE-38 oligo were inserted head-to-tail upstream of the TATA basal promoter regulating the expression of firefly luciferase. (B) The SRE-TATA-luciferase construct was cotransfected with a *Renilla* luciferase construct regulated by the HSV-TK promoter into HEK293 cells. 24 h after compound treatment, the ratio of firefly (F) to *Renilla* (R) luciferase activity was determined.

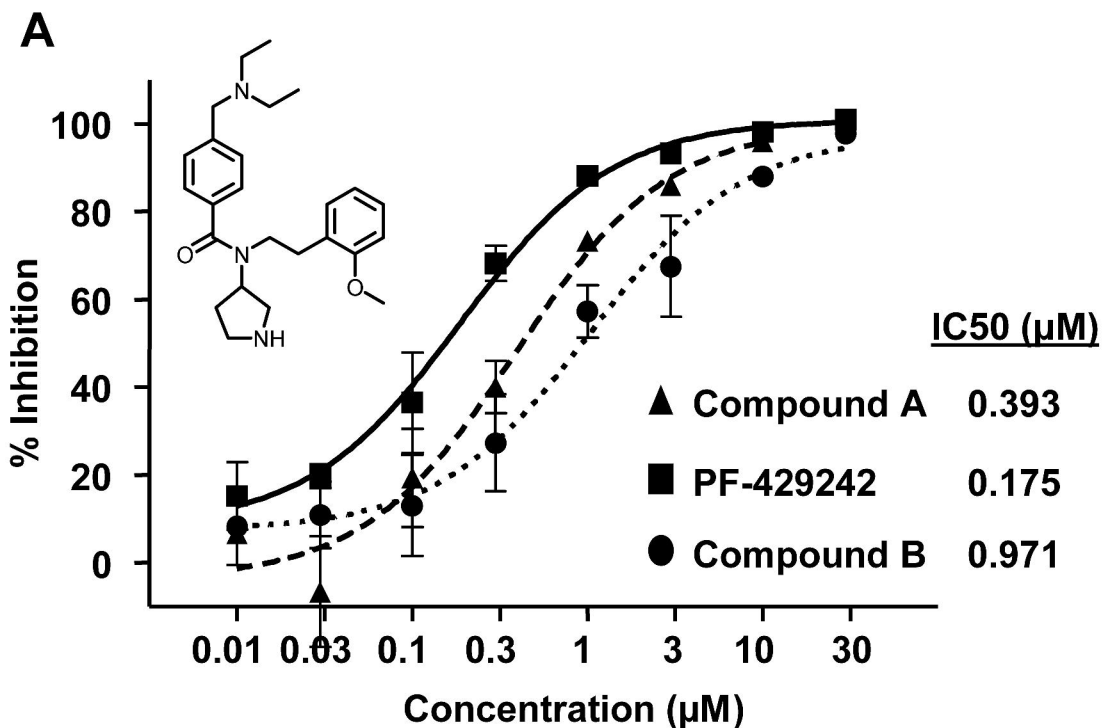
Relative SRE-target gene expression in compound treated cells (as represented by F/R) was assessed as a percentage of F/R in vehicle treated cells. The inhibitory profiles of PF-429242 and two related analogs (compounds C and D) are shown. Data are the average of triplicate determinations \pm SD. (C) The structures of PF-429242, Compound C, and Compound D.

Fig. 3. Inhibition of SREBP target gene expression and inhibition of lipid synthesis in HepG2 cells. HepG2 cells were cultured in delipidated serum (LPDS) and treated with PF-429242 at the indicated concentrations for 24 h. Inhibition of SREBP target gene expression by PF-429242 was determined by real-time quantitative PCR. (A) PF-429242 dose-related reduction of expression levels for fatty acid synthase (black bars) and HMG-CoA synthase (grey bars) relative to levels in vehicle-treated cells. Data are the average of triplicate determinations \pm SD. (B, C) PF-429242-induced effects on expression of LDL receptor and ABCA1, respectively, relative to vehicle-treated cells. Data are the average of triplicate determinations \pm SD. (D) Effect of PF-429242 treatment on cholesterol synthetic rate, as determined by [2- 14 C]acetate incorporation into cholesterol. Data are the average of triplicate determinations \pm SD.

Fig. 4. Inhibition of SREBP target gene expression and cholesterol and fatty acid synthesis in CD-1 mice. (A) Inhibition of SREBP target gene expression by PF-429242 was determined by real-time quantitative PCR. Six CD-1 male mice per group were dosed with vehicle (black bar) or PF-429242 at 10 mg/kg (grey bar) and 30 mg/kg (open bar) every 6 h for 24 h. Data are shown as mean \pm SD. ** $p < 0.01$ versus vehicle treated

group (student T-test). Inhibition of the synthesis of (B) cholesterol and (C) fatty acids by PF-429242 was determined by measuring the rate of [2-¹⁴C]acetate incorporation into cholesterol and fatty acids in CD-1 mice. Ten CD-1 male mice per group were dosed with vehicle or PF-429242 at 10 mg/kg and 30 mg/kg every 6 h for 24 h. Data are shown as mean \pm SEM. ***p<0.001 versus vehicle treated group (student T-test).

Fig. 1

**B**

Lane	1	2	3
10 $\mu\text{g/ml}$ cholesterol	-	+	-
1 $\mu\text{g/ml}$ 25-hydroxycholesterol	-	+	-
10 μM PF-429242	-	-	+

Membrane SREBP-2

Nuclear SREBP-2

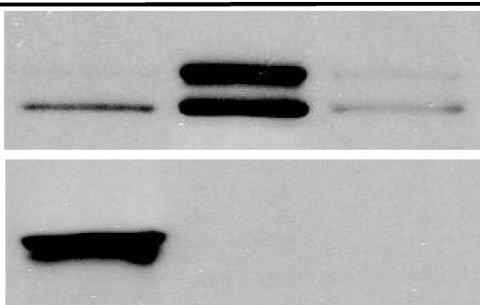
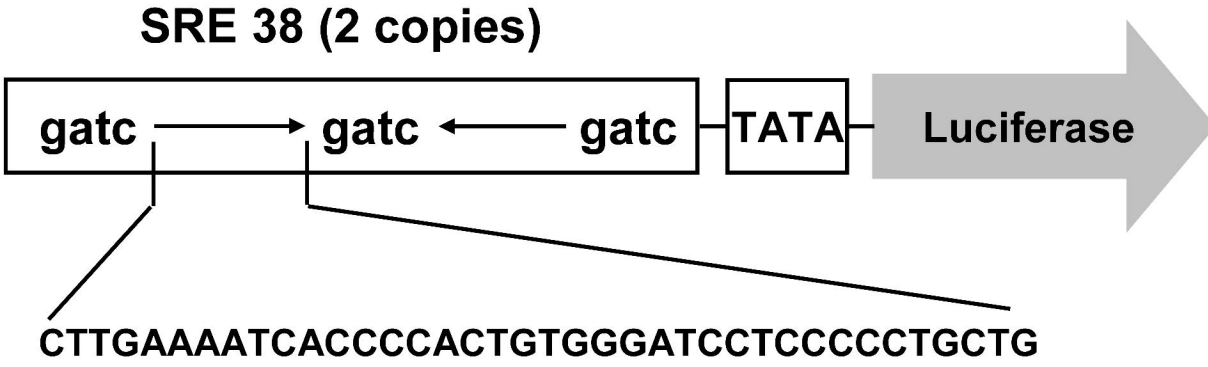
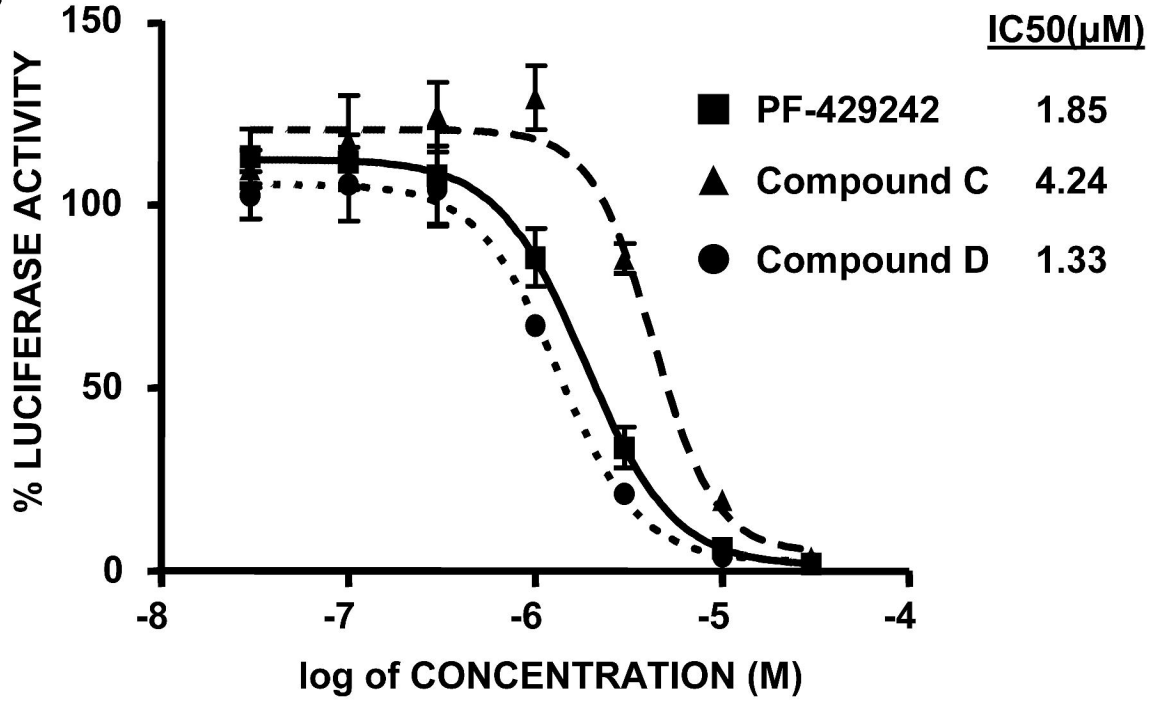


Fig. 2

A



B



C

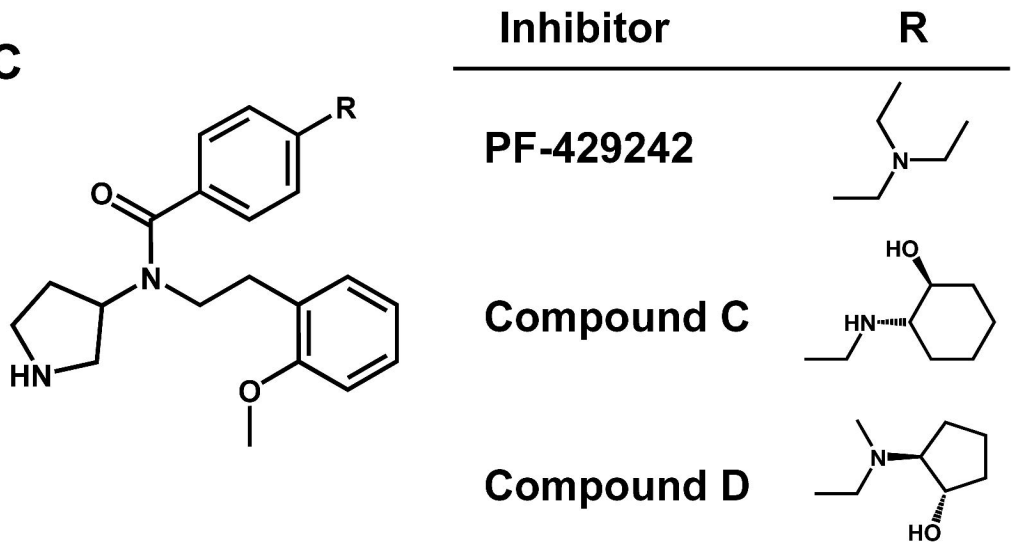


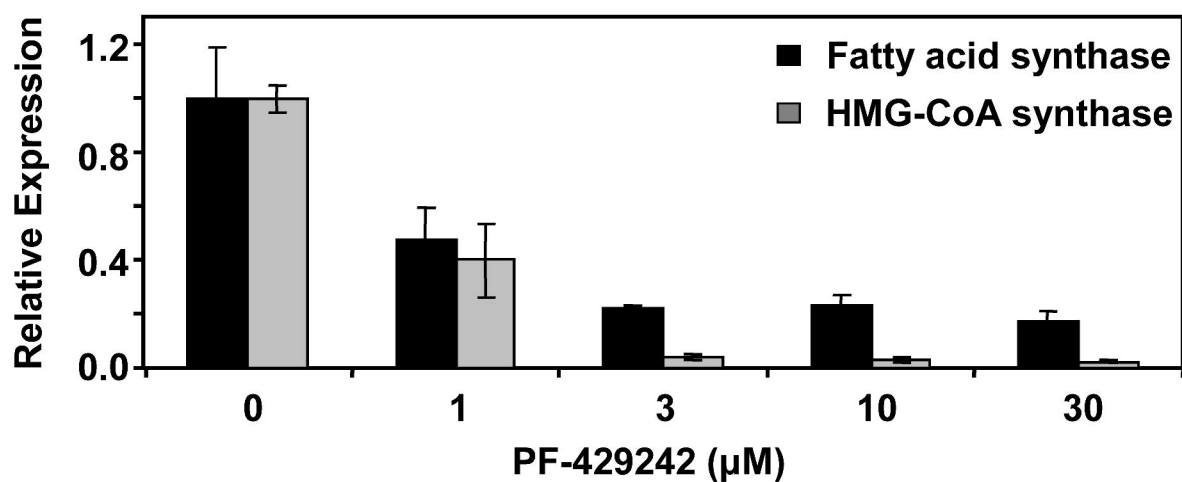
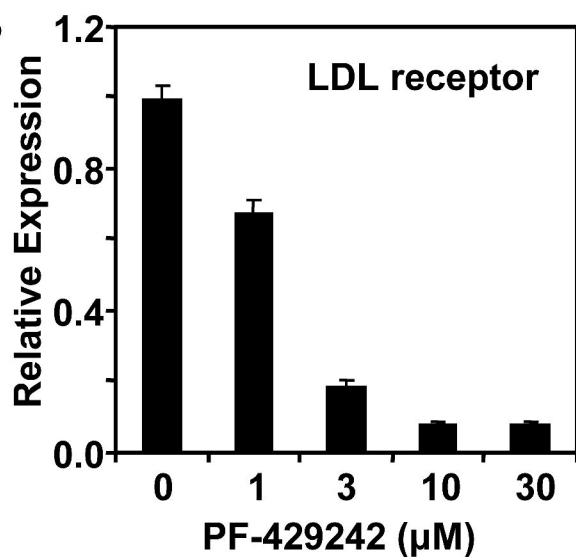
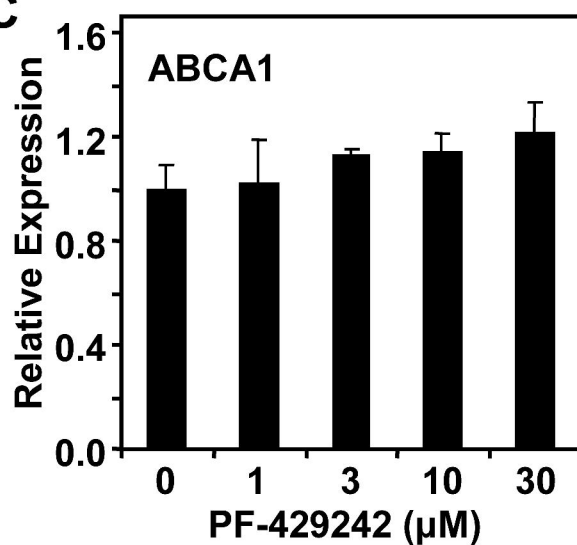
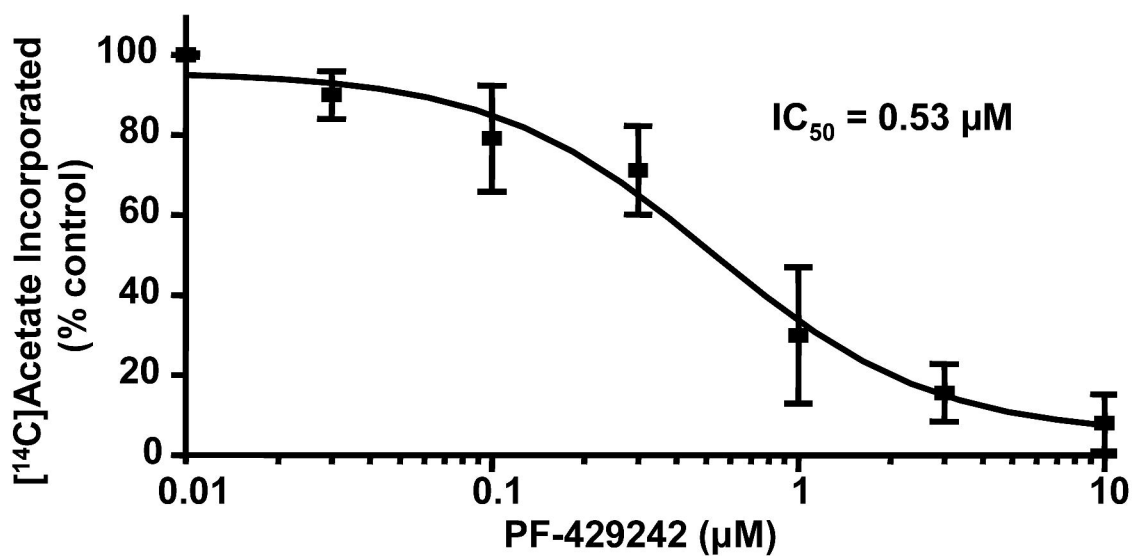
Fig.3**A****B****C****D**

Fig. 4

